A&A 516, A41 (2010)
DOI: 10.1051/0004-6361/200913563

Astronomy & Astrophysics

The evolution of an intra-cluster and intra-group stellar population

Their contribution to the stellar mass, their age, and their dynamics

W. Kapferer[1], S. Schindler[1], S. R. Knollmann[2], and E. van Kampen[3]

[1] Institute for Astro- and Particle Physics, University of Innsbruck, Technikerstr. 25, 6020 Innsbruck, Austria
e-mail: wolfgang.e.kapferer@uibk.ac.at
[2] Departamento de Física Teórica, Modulo C-XI, Facultad de Ciencias, Universidad Autónoma de Madrid, 28049 Cantoblanco, Madrid, Spain
[3] ESO, Karl-Schwarzschild-Strasse 2,85748 Garching bei Muenchen, Germany

Received 28 October 2009 / Accepted 30 March 2010

ABSTRACT

Aims. We investigate the properties of an intra-cluster stellar population (ICSP) and an intra-group stellar population (IGSP) as a function of time. We apply different criteria to separate between the stellar components residing in the galaxies and in the intergalactic spaces. In addition we investigate the rate of SNIa events in the ICSP/IGSP and the amount of ^{56}Fe produced by these events. Finally we compare the dynamics of the ICSP/IGSP with the stellar component residing in the galaxies.
Methods. By applying a combined N-body/hydrodynamic description (GADGET-2) with radiative cooling and a recipe for star formation and stellar feedback two different sized systems were calculated, i.e. galaxy cluster and galaxy groups. From these simulations extended halo catalogues were extracted with AHF: Amiga's Halo Finder. Together with the full information of all particles in the simulation several separation criteria between the ICSP/IGSP and the stellar component in the galaxies were investigated in detail.
Results. Applying different criteria to distinguish the stellar components inside and outside clusters/groups reveals different amounts of stellar mass present in the ICSP. We find that 7% to 40% of all stars belong to the ICSP in the galaxy cluster simulation depending on the applied separation criteria at redshift $z = 0$. The same separation criteria applied on a group simulation results in a 3% to 30% IGSP component compared to the total stellar mass in the system at redshift $z = 0$. Our investigation reveals a major difference between the gradient in the evolution of the ICSP and IGSP; the stellar mass present in the ICSP is increasing, whereas the fraction of stellar mass in the IGSP is decreasing in the same redshift regime. Applying simple SNIa rate estimates yields SNIa rates for the ICSP/IGSP of the order of 0.05 SNIa events per year in the ICSP and one order of magnitude lower for the IGSP, reflecting the different stellar masses in the ICSP/IGSP. The amount of ^{56}Fe-mass produced by the ICSP/IGSP SNIa is nearly two orders of magnitudes lower than observed values. The mean age of the stellar component populating the ICSP/IGSP is younger than the mean age of the stellar component in the galaxies. The maximum in the velocity distribution of the ICSP is shifted to lower velocities compared to the maximum in the velocity distribution of the stellar component in the galaxy cluster simulation. This reflects the high galaxy interaction rate present in the galaxy clusters. The difference gives us a measure for the dynamical state of the galaxy cluster/group.

Key words. methods: numerical – galaxies: interactions – galaxies: clusters: general – galaxies: general

1. Introduction

Observations of a diffuse stellar light between the galaxies in galaxy clusters have shown that the intra-cluster stellar population (ICSP) represents a substantial fraction of the total stellar population present in the galaxy clusters (Arnaboldi et al. 2002, 2003, 2004; Feldmeier et al. 2003; Gerhard et al. 2005; Mihos et al. 2005). The fraction of the ICSP to the total stellar population in a galaxy cluster seems to scale with the total mass of the system. Even in galaxy groups a diffuse component was detected (Sulentic & Lorre 1983; Moles, et al. 1998). More recent studies (Nishiura et al. 2000; White et al. 2003) have identified an intra-group stellar population (IGSP) in HCG 79 and HCG 90. In these systems 13% and 45% of the total light of the group in the B band corresponds to the IGSP, respectively. Zibetti et al. (2005) investigated the spatial distribution and colour of intra-cluster light (ICL) in 683 galaxy clusters in the redshift range between $z = 0.2$ and 0.3, selected from the first data release of the Sloan Digital Sky Survey. They found that on average the ICL contributes only a small fraction of the total optical emssion in a given cluster. Within a fixed distance of 500 kpc around the brightest cluster galaxies (BCDs) the average fraction is 10.9 ± 5.0 per cent. Furthermore the authors claim that the ICL is aligned with and more flattened than the BCG itself and that the surface brightness of the ICL correlates both with the BCG luminosity and the richness of the cluster. Krick & Bernstein (2007) investigated the ICL in a sample of 10 galaxy clusters and found that a cD galaxy in the cluster yields centrally concentrated ICL profiles. They conclude that their finding is consistent with ICL either forming from galaxy interactions at the the centre of the clusters or at high redshifts in groups which will merge in the centre at lower redshifts. On the scale of galaxy groups Da Rocha et al. (2008) found by investigating three compact groups, HCG 15, 35 and 51 that 19, 15 and 26 per cent of the total light in these groups are in the diffuse component, with colours that are comparable with old stellar populations.

The origin and the evolution of the ICSP is currently under debate. The ICSP could be produced by tidal stripping and disruption of galaxies at their passage through the dense central region of the galaxy cluster (Byrd & Valtonen 1990; Gnedin 2003). Maybe the ICSP was formed by tidal stripping of galaxies at the very initial formation of the galaxy cluster (Merritt 1984).

Another proposed process are high-velocity galaxy encounters in the dense cluster environment (Moore et al. 1996) or galaxy mergers (Kapferer et al. 2005; Murante et al. 2007), which can redistribute stellar matter up to large radii around the interacting systems. As ram-pressure stripping is able to trigger star formation in the stripped gaseous wake (Kronberger et al. 2008; Kapferer et al. 2008, 2009) this process forms stars directly in the intra-cluster space.

Besides the origin of the ICSP several numerical investigations of their properties were carried out. First approaches were pure dark matter simulations in which the dark matter particles acted as tracer particles for a supposed stellar component (Napolitano et al. 2003). Λ cold dark matter (CDM) cosmological hydrodynamic simulations were carried out by Murante et al. (2004, 2007) to quantify the amount and distribution of the ICSP in a set of galaxy clusters. Willman et al. (2004) found the fraction of the ICSP to the total stellar population grows with the infall of groups during the formation of the galaxy cluster. The properties of intra-group stars in galaxy groups were investigated in detailed TreeSPH simulations by Sommer-Larsen (2006). The simulations included a star-formation recipe, chemical evolution with non-instantaneous recycling, metallicity-dependent radiative cooling, strong star-burst driven galactic super-winds and effects of a meta-galactic ultraviolet field. The author found that intra-group (IG) stars contribute 12–45 per cent of the total group B-band luminosity at $z = 0$. In addition it was found that the IG stars in fossil groups are older compared to the IG stars in the "normal" groups. Furthermore the author could show that the mean iron abundance of the IG stars is slightly sub-solar in the central parts of the groups and decreases to about 40 per cent solar at half virial radius. Furthermore, the expected number of planetary nebulae in fossil groups was published by Sommer-Larsen (2006), which is of the order of 500 at projected distances between 100 and 1000 kpc from the first ranked galaxy.

By applying an extensively tested analytical model for subhalo infall and evolution together with empirical constraints from galaxy survey data to set the stellar mass in each accreted subhalo, which is added to the difusse light, Purcell et al. (2007) investigated dependencies of the diffuse stellar light on the mass properties of the host system. The authors found that intrahalo light is in the range from 0.5% to 20% from small galaxy halos ($\sim 10^{11}\ M_\odot$) to poor groups ($\sim 10^{13}\ M_\odot$). Beyond the group scale the trend in the fraction of intrahalo light flattens and increases weakly from a fraction of ∼20% in poor galaxy clusters ($\sim 10^{14}\ M_\odot$) to ∼30% in massive clusters ($\sim 10^{15}\ M_\odot$). Purcell et al. (2007) found that the intracluster light is mainly liberated from massive galaxies $M_\star \sim 10^{11}\ M_\odot$.

In this work we investigate different definitions for the ICSP or intra-group stellar population (IGSP). Also the difference between the ICSP/IGSP and the stellar component with respect to dynamics and age is studied. Therefore we applied two high-resolution Λ cold dark matter (CDM) cosmological hydrodynamic simulations with constrained initial conditions to investigate the diffuse stellar component in two very different systems, an intermediate mass galaxy cluster and a simulation volume in which several massive groups of galaxies are formed. Furthermore we estimate the amount of SN Ia events in the intergalactic space and their importance for the enrichment of the intra-cluster/inter-galactic medium. In addition we investigate the dynamics of the ICSP/IGSP with respect to the dynamics of the galaxies and the dark matter component.

The investigation of the diffuse stellar component in galaxy clusters and groups sheds more light on the formation history of these systems. Furthermore the interaction between the ICSP/IGSP and its environment is poorly understood and due to observational limits not investigated yet.

The paper is structured as follows. After introducing the numerical setup we give basic properties of the simulated systems. The different selection criteria for the ICSP/IGSP are presented Sect. 4. In Sect. 5 we give the dependence of the fraction of the ICSP/IGSP as a function of definitions, similar to the procedure observers would apply. The dynamics of the ICSP/IGSP is compared to the dynamics of the galaxies and the dark matter components of the systems in Sect. 6. Finally the conclusions and discussion on the results are given in Sect. 7.

2. Numerical setup

The simulations were carried out with the *N*-body/SPH code GADGET-2 developed by Springel (see Springel 2005 for details). The code treats the gas of the galaxies and the surrounding gas by smoothed particle hydrodynamics (SPH Gingold & Monaghan 1977; Lucy 1977). The collisionless dynamics of the dark matter and the stellar component is modelled by an *N*-body technique. Additional routines for cooling, star formation (SF), stellar feedback, and galactic winds are included as described in Springel & Hernquist (2003). The structure of GADGET-2 is based on the TreeSPH code Hernquist & Katz (1989), where gravitational interactions are calculated by a hierarchical multipole expansion, and the gas dynamics is treated by means of smoothed particle hydrodynamics (SPH). The gas particles are distinct tracer particles with an additional kernel interpolation to describe continuous fluid quantities. Gadget2 defines the thermodynamic state of each fluid element in terms of entropy per unit mass and conserves both energy and entropy. Discontinuities in gaseous matter generate entropy, which is treated by an artificial viscosity term in the SPH scheme. The most important component of the scheme is the density estimate at the position of each gas tracer particle. An adaptive smoothing length h_i for each particle is defined in a way that the corresponding kernel volume contains a constant mass for the estimated density. The smoothing length and the corresponding estimated density is calculated by $\frac{4\pi}{3} h_i^3 \rho_i = N_{\rm sph} \overline{m}$ where $N_{\rm sph}$ is the number of neighbours taken into account, and $\overline{m}$ is the corresponding average particle mass. Details on the equation of motion and the thermodynamics can be found in Springel et al. (2005). To model star formation we applied the so called "hybrid" method for star formation and feedback which was introduced by Springel & Hernquist (2003). In this approach, cold gas clouds coexist in pressure equilibrium with a hot ambient gas. With the average density of the stars ρ_*, the cold gas $\rho_{\rm c}$ and the hot medium $\rho_{\rm h}$, the total gas density in the disk can be written as $\rho = \rho_{\rm h} + \rho_{\rm c}$. Due to the finite number of particles in our simulations ρ_* and ρ represent averages over regions of the inter-stellar medium (ISM). The central assumption in the approach is the conversion of cold clouds into stars on a characteristic timescale t_* and the release of a certain mass fraction β due to supernovae (SNe). This relation can be expressed as

$$\frac{{\rm d}\rho_*}{{\rm d}t} = \frac{\rho_{\rm c}}{t_*} - \beta \frac{\rho_{\rm c}}{t_*} = (1-\beta)\frac{\rho_{\rm c}}{t_*} \cdot \tag{1}$$

As the released material from SNe is hot gas, the cold gas reservoir decreases at the rate $\rho_{\rm c}/t_*$. In this picture, β gives the mass fraction of massive stars (>8 $M_\odot$). As in Springel & Hernquist (2003) we adopt $\beta = 0.1$ assuming a Salpeter IMF with a slope of –1.35 in the limits of 0.1 $M_\odot$ and 40 $M_\odot$. Furthermore each supernova event releases energy of 1×10^{51} erg into the ambient

Table 1. Properties of the particles in the simulations.

	Particle mass dark matter $M_\odot\,h^{-1}$	Particle mass gas $M_\odot\,h^{-1}$	Particle mass stellar $M_\odot\,h^{-1}$	length softening [kpc h^{-1}]
group	1.5×10^8	1.7×10^7	7.8×10^6	4
cluster	1.4×10^8	1.7×10^7	7.3×10^6	4

Notes. Particle mass resolution and softening length for the simulations.

medium. This leads to an average return of $\epsilon = 4\times10^{48}$ erg $M_\odot^{-1}$. The ambient hot medium is heated and evaporates the cold clouds inside the hot bubbles of exploding SNe. The total mass of clouds evaporated can be written as

$$\frac{\mathrm{d}\rho_\mathrm{c}}{\mathrm{d}t}|_{EV} = -A\beta\frac{\rho_\mathrm{c}}{t_*}\,. \tag{2}$$

The evaporation process is assumed to be a function of the local environment with an efficiency A $\propto \rho^{-4/5}$ (McKee & Ostriker 1977). The minimum temperature the gas can reach due to radiative cooling is about 10^4 K. The energy balance per unit volume is $\epsilon_{UV} = \rho_\mathrm{h} * u_\mathrm{h} + \rho_\mathrm{c} * u_\mathrm{c}$ ($u_\mathrm{h,c}$ energies per unit mass of the cold and hot gas). These assumptions lead to self-regulating star formation due to the conversion of cold gas into stars and the feedback of hot gas into the reservoir of the hot ambient medium, which can cool due to radiative cooling to cold clouds. For a more detailed description of the feedback routine see Springel & Hernquist (2003).

3. Properties of the modelled systems

In order to investigate the properties of the ICSP/IGSP and their evolution we simulated two different systems, an intermediate massive galaxy cluster and a group of galaxies. The initial conditions were created using the constrained random field method of Hoffman & Ribak (1991), as implemented by van de Weygaert & Bertschinger (1996). The computational domains were represented by a periodic boundary box with 32 Mpc h^{-1} side length at a starting redshift of $z = 99$. The extent of the box was chosen to be well above the size of the cluster in the centre of the box. However, the fundamental mode for this box is approximately 5 h^{-1} Mpc, close to the size of the cluster, hence this is the smallest box that still allows the cluster to evolve properly towards its final overdensity. Even though the cluster models do lack the effect of the surrounding large-scale structure distribution, e.g. tidal fields, we feel that for case studies, i.e. individual cluster simulations such as presented in this paper, this is not an important drawback, and the advantage of being able to simulate at a higher resolution easily justifies our choice for the smallest possible boxsize. The simulations employed 256^3 dark matter and 256^3 gas particles. In Table 1 the mass resolution of the different components and the softening length are given. For the galaxy group simulation in a total of 174 177 timesteps and for the galaxy cluster simulation a total of 472 698 timesteps were calculated, respectively. Based on the detailed resolution analysis of Murante et al. (2007) we can conclude that the resolution presented in this work is sufficient to allow a detailed investigation of the ICSP/IGSP. In Fig. 1 the distribution of the different components of the two simulated systems at a redshift $z = 0$ centred on the most massive halo found in the computational domain is shown. In the top panel the temperature of the gas in a 10 Mpc h^{-1} area around the centre of mass is shown, in the middle panel the dark matter distribution in the same area and in the the lower panel the stellar distribution again in the same region is drawn. The evolution of the virial mass within the most massive halo found in the the simulation in the redshift regime $0 \le z \le 1$ is given in Fig. 2.

4. Selection criteria for the intra-cluster stellar population

As the full dynamical knowledge of the stellar component in the systems investigated in this work is not accessible to observers, we follow a different approach compared to previous works (e.g. Murante et al. 2004, 2007): We separate the ICSP/IGSP from the stellar component in the galaxies by means of the distance of a stellar particle to all identified haloes in the simulations within a 2 Mpc h^{-1} sphere around the cluster/group centre. We do not make any distinction between main group/cluster halos and subhalos. This implies that central galaxies and satellite galaxies are treated with the same scaling relations for separating the galactic from ICSP/IGSP stars. This is a different approach compared to the work of e.g. Sommer-Larsen et al. (2005) and Sommer-Larsen (2006), where a tidal radius limit was applied to define the intracluster stars. In a forthcoming work these different scaling relations for group/cluster halos and sub-halos and their influence on the amount of ICSP/IGSP will be studied.

As a first step in extracting the ICSP/IGSP a halo finder algorithm was applied. The (sub)halo properties for 393 different time-steps, equally distributed along the time axis of the simulations, were extracted with AHF (AMIGA Halo Finder, Knollmann & Knebe 2009). For each identified (sub)halo several properties of the different components in the simulation – total matter, gaseous matter and stellar matter – were extracted. Among the different parameters are halo mass, virial radius, dynamical properties like virial velocities, just to mention some.

A detailed description of AHF is given in the code description paper Knollmann & Knebe 2009), but for convenience we will provide a brief summary of the mode of operation below. By virtue of the adaptive mesh hierarchy employed to sample the density field, AHF locates overdensities as prospective halo centers. The local potential minima are computed for each of these density peaks and, treating the prospective halo in isolation, the gravitationally bound particles are determined. Only peaks with at least 20 bound particles are considered as haloes and retained for further analysis.

For each halo we computed the virial radius r_vir, that is the radius r at which the density $M(<r)/(4\pi r^3/3)$ drops below $\Delta_\mathrm{vir}\rho_\mathrm{back}$. Here ρ_back is the cosmological background density. The threshold Δ_vir was computed using the spherical top-hat collapse model and is a function of both cosmological model and time. Subhaloes are defined as haloes which lie within the virial region of a more massive halo, the so-called host halo. As subhaloes are embedded within the density of their respective host halo, their very own density profile usually shows a characteristic upturn at a radius $r_t \le r_\mathrm{vir}$, where r_vir would be their actual (virial) radius if they were found in isolation. We used this "truncation radius" r_t as the outer edge of the subhalo.

Hence (sub-)halo properties (i.e. mass, density profile, velocity dispersion, rotation curve) were calculated using the

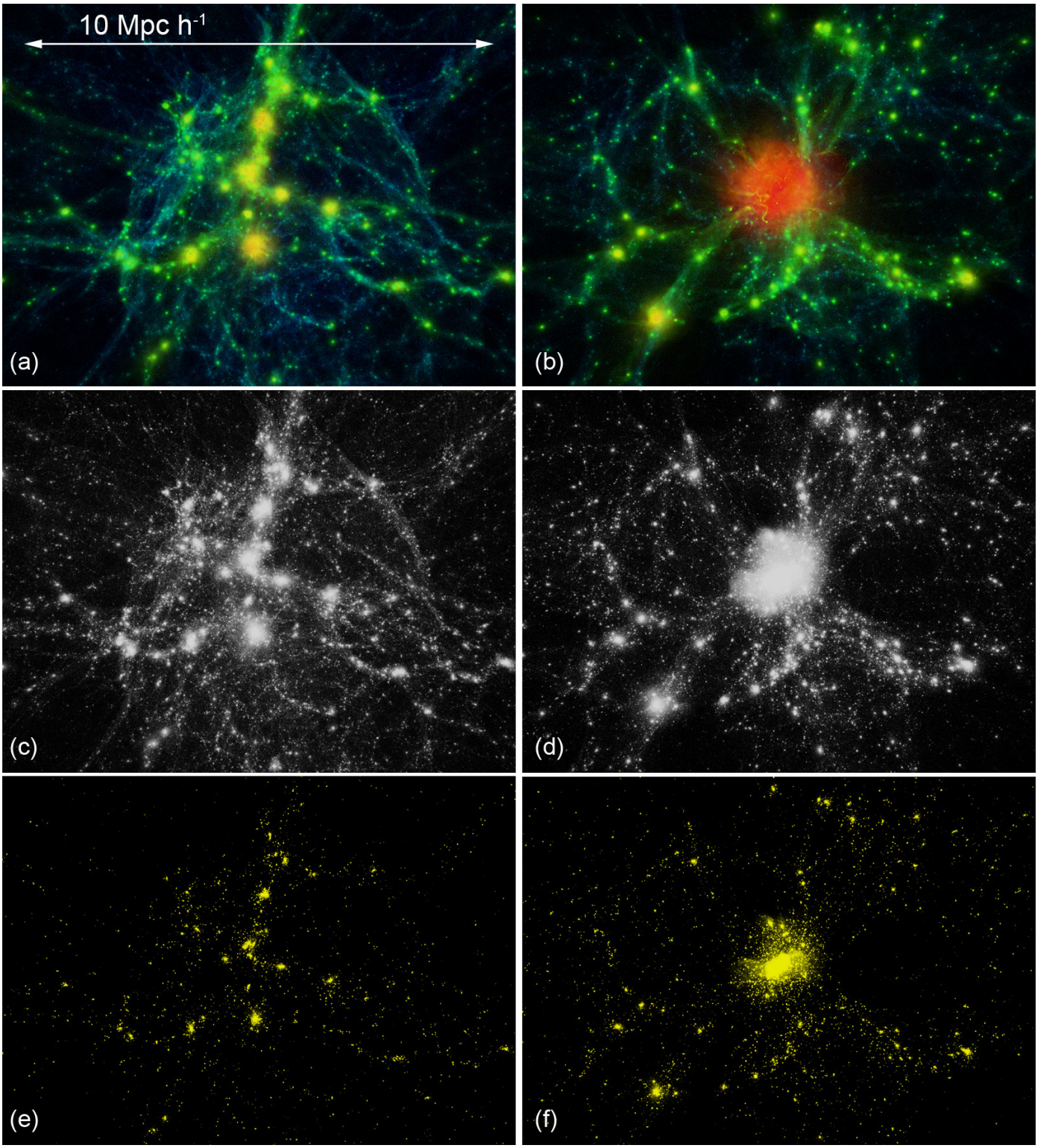

Fig. 1. Distribution of the different components, i.e. gas, stellar matter and dark matter, in the simulated systems at redshift $z = 0$. In the top panel the left side **a)** shows the gas temperature in the galaxy group, whereas the right side **b)** shows the same quantity for the galaxy cluster. In the middle panel the dark matter distribution in the same area is shown for the group **c)** and the galaxy cluster **d)**. In the lower panel the distribution of the stars in the galaxy group **e)** and in the galaxy cluster **f)** in the same region is given.

gravitationally bound particles inside either the virial radius $r_{\rm vir}$ for a host halo or the truncation radius r_t for a subhalo[1].

In Figs. 3 and 4 the virial and stellar mass functions of the two simulations are plotted at redshift $z = 0$. The structure formation

[1] Note that we did not remove subhalo particles from their respective host halo unless they were gravitationally unbound.

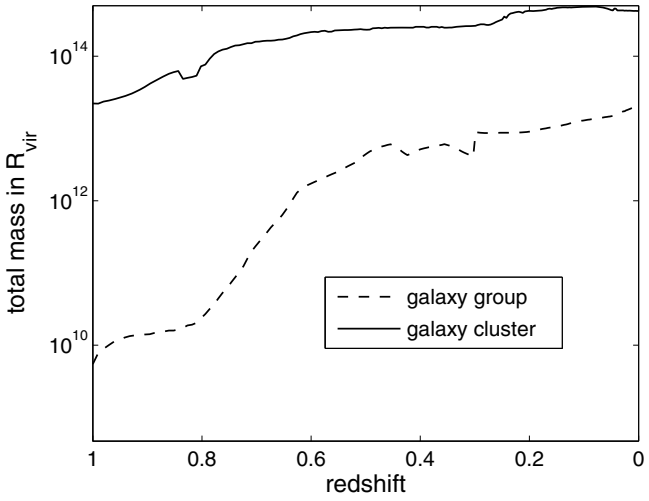

Fig. 2. The evolution in the redshift range $0 \leq z \leq 1$ of the total mass within the virial radius of the most massive halo residing in the simulations.

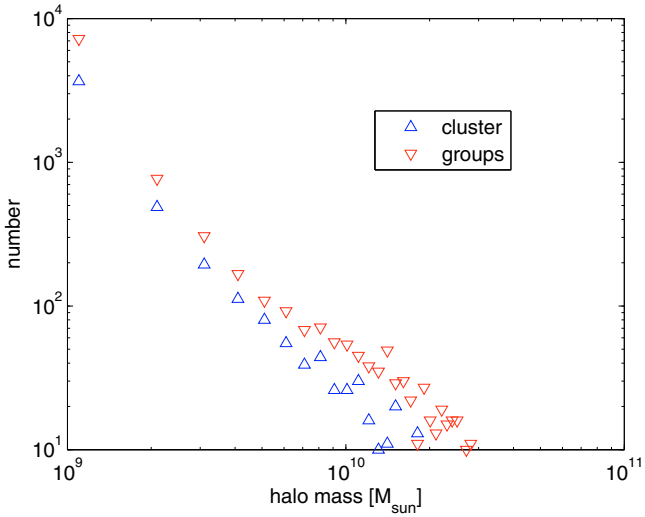

Fig. 4. Histogram of stellar mass present in haloes in the simulations at redshift $z = 0$.

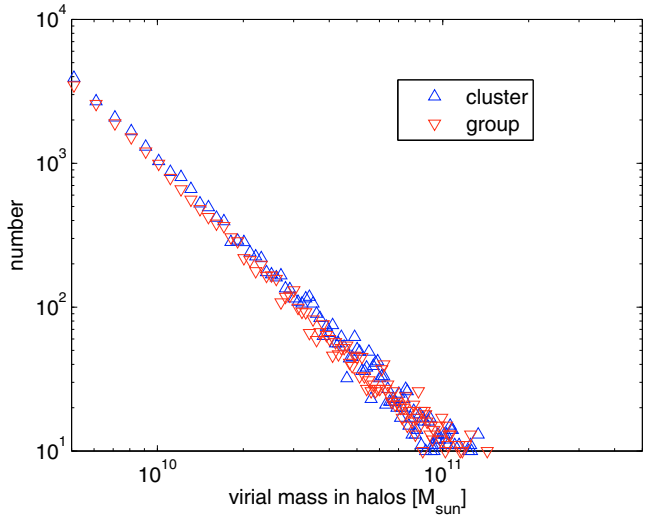

Fig. 3. Histogram of the virial mass of haloes found in the simulations at redshift $z = 0$.

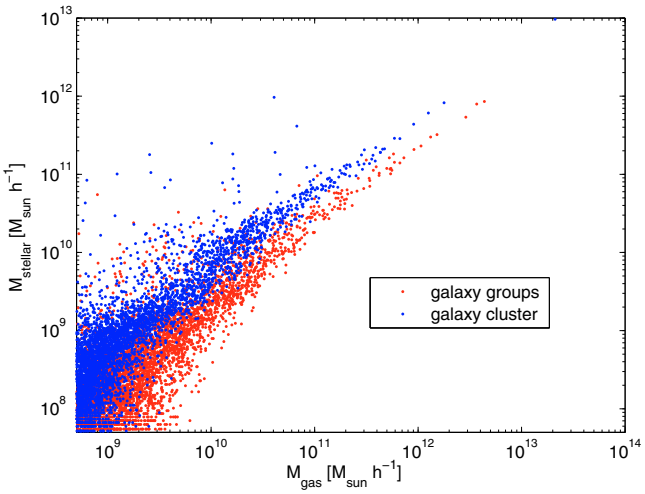

Fig. 5. The gas mass of all haloes found in the simulations at redshift $z = 0$ against the stellar mass present in the haloes.

in the galaxy cluster simulation does suppress star formation in comparison to the galaxy group simulation. In Fig. 5 a scatter plot of the mass of stars found in all halos against the stellar mass in the halos is given for redshift $z = 0$. In the plot the resolution within the simulations can be seen. Within the smallest bound halos a stellar population in the range of several 10^7 $M_\odot$ is present in both systems. The influence of a hot intra-cluster medium (ICM) and high merger rates in galaxy clusters on the gas content in the halos can also be seen in Fig. 5. On average the halos have less gas content for a given stellar mass content. Given full information of all the particles throughout the computational domain and the properties of the bound structures by means of the halo extraction routine, several separations criteria for the ICSP/IGSP were applied. The criteria are as follows.

The first two are simply fractions of the virial radius. Criterion 1: If a stellar particle distance to all found haloes in the simulation is larger then 0.1 $R_{\rm vir}$ the particle is flagged as a member of the ICSP/IGSP. Criterion 2: If a stellar particle distance to all found haloes in the simulation is separated more than 0.5 $R_{\rm vir}$ the particle is flagged as a member of the ICSP/IGSP (Criterion 2).

For each halo we determined if the gas mass is less than 10% compared to the stellar mass for a given time. If this criterion was fulfilled the halo was treated as if it would harbour an elliptical or S0 galaxy and consequently an effective radius iswascalculated as described in Chiosi & Carraro (2002) for the corresponding halo. In Chiosi & Carraro (2002) two mass-radius relations for elliptical systems with stellar masses $M \geq 10^{10}$ $M_\odot$ and $M < 10^{10}$ $M_\odot$ were derived respectively. The effective radius for the massive systems was calculated by $R_{\rm e} = 21.908 \times M_{\rm stellar}^{0.6}$ [kpc] and for the less massive systems by $R_{\rm e} = 3.014 \times M_{\rm stellar}^{0.218}$ [kpc]. If haloes have a gas to stellar matter fraction higher than 0.1 the halo was considered to harbour a late-type galaxy. In this case a disc radius $R_{\rm d}$ for the corresponding halo was derived as proposed in Burkert & D'Onghia (2004). They propose to calculate by $R_{\rm d}$ by $R_{\rm d} = 8.5 \frac{\lambda'}{0.035} \frac{v_{\rm c}}{200\ {\rm km\,s^{-1}}}$ kpc. Where λ' is the dimensional spin parameter of the halo as proposed by Bullock et al. (2001) and $v_{\rm c}$ is the peak velocity of the dark matter rotation curve.

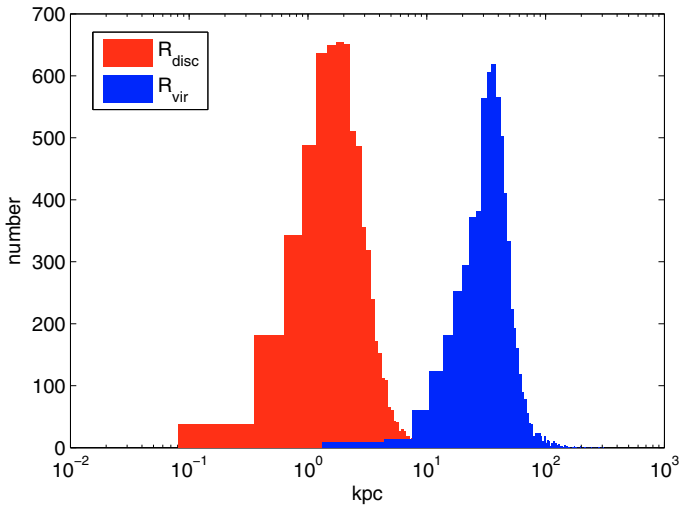

Fig. 6. Histogram of the disc length and the virial radii for late type galaxies in the whole galaxy cluster simulation volume.

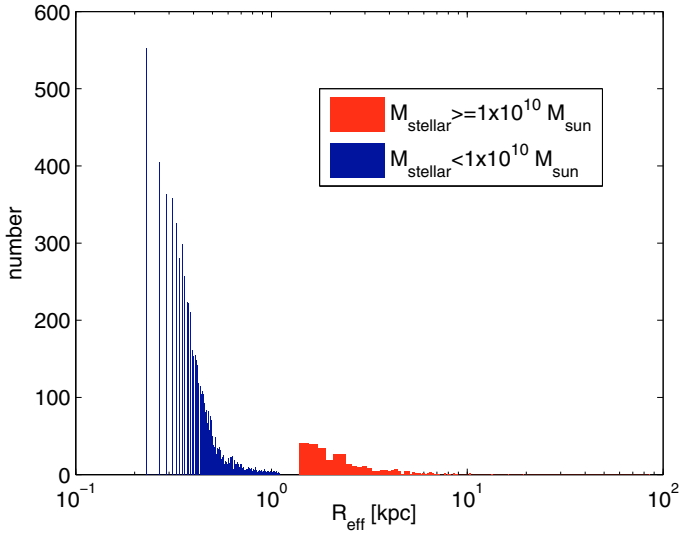

Fig. 7. Histogram of the effective radii for all early type galaxies in the whole galaxy cluster simulation volume.

Given these two parameters R_e and R_d for each bound halo three different criteria for counting a stellar particle to the ICSP/IGSP were applied. Criterion 3: If the distance of a stellar particle to all haloes in the simulation is larger than 3 R_e for haloes harbouring elliptical systems and 6 R_d for haloes harbouring late-type systems, the stellar particle is added to the ICSP. Criterion 4 and 5: If the separation is larger than 5 R_e and 8 R_d or if the distance is larger than 7 R_e and 10R_d the particle is counted to be a member of the ICSP/IGSP. In Figs. 6 and 7 the histograms of the disc scale length, effective radii and virial radii for early and late type galaxies in the whole galaxy cluster simulation volume at redshift $z = 0$ is shown. For a given galaxy with 10% gas mass the difference between R_e and R_d is typically very small.

In Table 2 the criteria are summarised. With these criteria we were able to obtain a more realistic determination if the ICSP/IGSP compared to observations, which are inherently separation-based criteria.

Table 2. Separation criteria for stellar particles belonging to the ICSP.

Criterion	1	2	3	4	5
R_{vir}	0.1	0.5	–	–	–
R_d	–	–	6	8	10
R_e	–	–	3	5	7

5. Properties of the intra-cluster stellar population

Applying the selection criteria for stellar particles presented in the last section allowed us to derive several properties of the ICSP/IGSP. In Figs. 8 and 9 the stellar surface-density maps for all separation criteria are shown for the galaxy cluster and galaxy group simulations at redshift $z = 0$. Obviously the simple separation criterion of 0.1 R_{vir} results in the most massive ICSP/IGSP component. Note that in Figs. 8 and 9 the remaining complementary stellar component in the galaxies is shown in white.

Increasing the separation from criterion 1 to criterion 2 (0.5 R_{vir}) leads to a much less massive ICSP/IGSP component. The other separation criteria, applying the disc-scale length R_d and the effective radius R_{eff} shows the expected behaviour of an increasing amount of ICSP/IGSP with smaller separation. The features at the edges of the major axis of the stellar component in the subclusters seen in the ICSP are a direct result of the fact that along this axis more galaxies are present.

The evolution of the stellar mass in the ICSP/IGSP due to the different separation criteria is given in Fig. 10.

The largest stellar mass in the ICSP/IGSP yields the separation criterion 1 (0.1 R_{vir}), the minimum amount of stellar mass can be found in the ICSP by applying separation criterion 2 (0.5 R_{vir}). The criteria 3–5 result in a steady decrease of mass in the ICSP/IGSP, as can be seen in the ICSP surface density maps presented in Fig. 8. Another interesting behaviour regarding the evolution of the stellar mass in the ICSP/IGSP can be seen in Fig. 10. After each merger event, which is established as a local maximum in the mass in the ICSP/IGSP the stellar mass in the ICSP/IGSP decreased afterwards. The reason for this is the dynamics of the stellar particles, which represent the ICSP/IGSP. After the structures interacted, the generated ICSP/IGSP started to relax dynamically, leading to a decrease in the mass of the ICSP/IGSP. Especially in the galaxy cluster simulation the temporary decrease of the stellar mass in the ICSP after a minor merger event at $z \sim 0.9$ is visible. Comparison of the ratio between the mass in the ICSP/IGSP to the total stellar mass and their evolution is shown in Fig. 11. Different separation criteria lead to different ratios in the range of 40% and 10% for the galaxy cluster system and 30% and 3% for the less massive galaxy group system at redshift $z = 0$. Again the increase of mass in the ICSP/IGSP after each major merger event is followed by an decrease due to violent relaxation. This oscillating behaviour was also found by Rudick et al. (2006). A striking difference between the two systems is the overall gradient. Whereas the relative IGSP is decreasing in the galaxy group simulation, the fraction of stellar mass present in the ICSP increases in the galaxy cluster system with time, although the virial mass is increasing in both systems. The explanation is found in the higher merger rates with higher velocities in galaxy clusters compared to the galaxy group. Furthermore high velocity encounters are able to accelerate stellar particles from the centres of the haloes to the surroundings (Kapferer et al. 2005), leading to a younger ICSP compared to the IGSP. It seems that the strength and the amount of galaxy interaction in galaxy groups are not sufficient to balance the violent relaxation over long timescales, leading

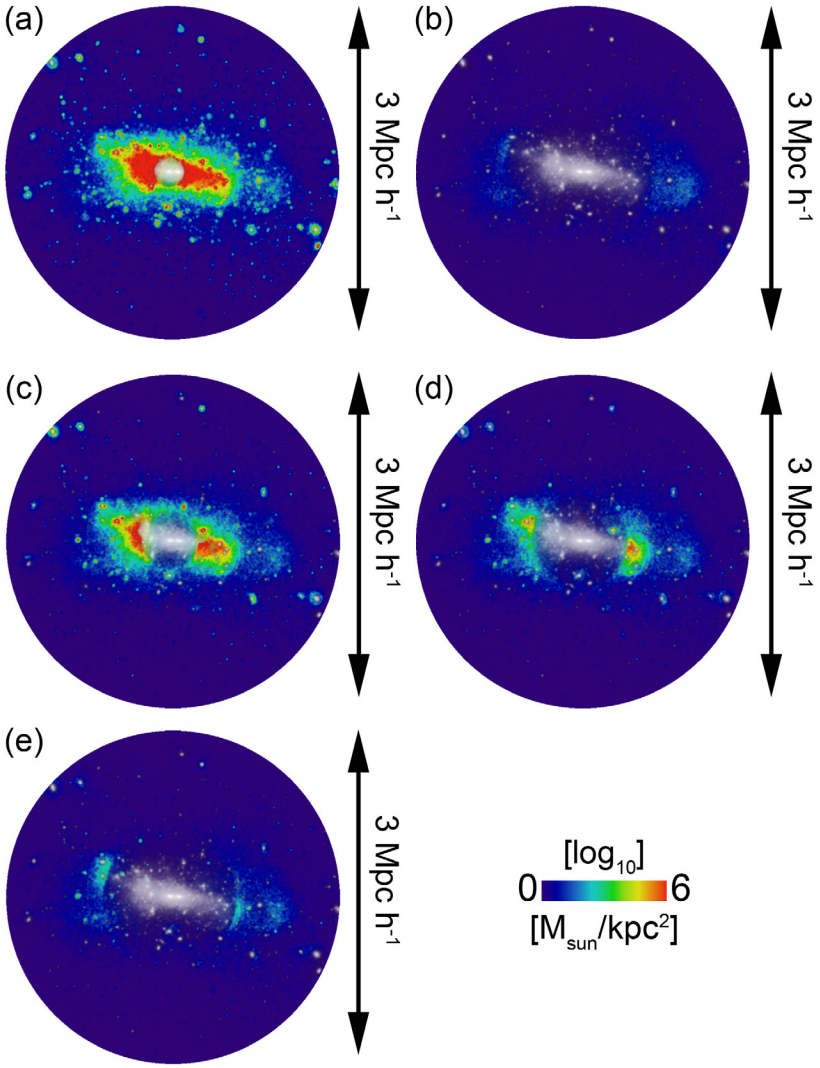

Fig. 8. Stellar surface-density for the intra-cluster stellar population (coloured map) and the stellar population in the galaxies (white to opaque colour map) for the different separation criteria for the galaxy cluster system at redshift $z = 0$. **a)**-criterion 1; **b)**-criterion 2; **c)**-criterion 3; **d)**-criterion 4; and **e)**-criterion 5.

to a decrease of the IGSP with redshift. The IGSP fraction at $z = 1$ is very high for the applied selection criteria. The reason for this behaviour is the merging of galaxies in the group environment. These mergers have lower relative velocities than in the galaxy cluster environment. The redistribution of matter for low relative velocity interactions is more effective (Kapferer et al. 2005), therefore leading to higher IGSP fractions.

In Fig. 12 the evolution of the total star-formation rate in the cluster and group simulation volume is shown. The group simulation does form stars at the same rate as the cluster simulation in the redshift range $z \sim 1$ to $z = 0$. This nicely reflects the star-formation decrease in galaxy clusters and does explain why the evolution of the fraction of diffuse light in the group simulation does not show a strong gradient as the cluster simulation. New stars in the galaxies are formed at a relatively higher rate. The decrease of the fraction of diffuse light in the group simulation in the redshift regime between $z = 1$ and $z = 0$ is partly caused by a lower merger rate: The group simulation exhibits a less pronounced galaxy merger rate compared to the cluster simulation. In addition, the fraction of diffuse light is decreasing because new stars are formed in the group galaxies, leading to a net decrease in the diffuse light component.

In galaxy clusters galaxy interactions at high-velocities, at a high rate, are much more common than in galaxy groups. Therefore the mean age of the ICPS is older than the mean age of the IGSP, because stellar particles that fall back on the merged haloes are again accelerated by a upcoming interactions. Furthermore the mean age of the diffuse stellar component should vary more strongly in galaxy groups than in galaxy clusters due to individually resolved galaxy interactions. In addition the stronger variation in the mean age in the IGSP depends on the star-formation history of the system. As there are more stars produced in the galaxy group simulation relative to the cluster simulation per stellar mass present in the system, the ratio of the mean ages in the galaxies and the diffuse component shows more scatter. In the galaxy cluster simulation the ages in the diffuse component are more comparable to the ages of the stars in the galaxies, because the star formation is truncated at earlier epochs. So the stars which will be distributed into the diffuse component have comparable ages, and therefore the scatter is much lower. In Fig. 13 this behaviour is clearly visible. On average the ICSP is 10% younger compared to the stellar component present in the bound structures in the galaxy cluster system, and in the IGSP the stellar component is 20% younger compared to the stellar component in the galaxies. Note that this result shows no strong dependency on the applied separation criteria. The evolution of the ICSP/IGSP surface density is shown in Fig. 14. Due to the complex dynamics in many interactions

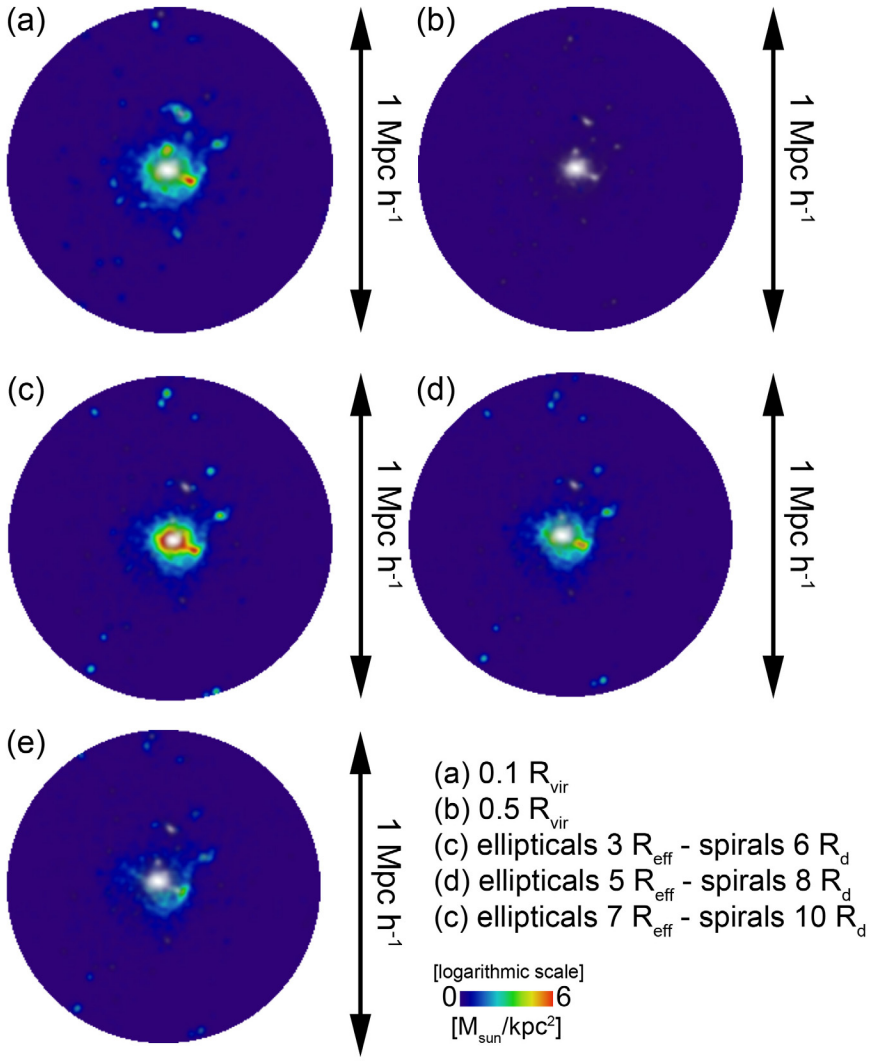

Fig. 9. Stellar surface-density for the intra-group stellar population (coloured map) and the stellar population in the galaxies (white to opaque colour map) for the different separation criteria for the galaxy cluster system at redshift $z = 0$. **a)**-criterion 1; **b)**-criterion 2; **c)**-criterion 3; **d)**-criterion 4; and **e)**-criterion 5.

present at the same time in the dense environment in a galaxy cluster, the ICSP distribution is very inhomogeneous.

In the galaxy-group system inhomogeneities are not as pronounced as in the galaxy-cluster system, due to the lower energies involved in the interactions compared to the galaxy-cluster system.

5.1. The SN Ia rate in the ICSP/IGSP

As supernova type Ia (SN Ia) are supposed to occur a long time after the progenitor stars were formed compared to core collapse supernovae type II (SN II), SN Ia are the dominant group in the ICSP/IGSP as the progenitor stars had enough time to travel from the places of formation into the intergalactic spaces. Observational evidence for intergalactic SN Ia are given in e.g. Gal-Yam et al. (2003).

By including a simple estimate for the number of SN Ia in our ICSP/IGSP extraction routines, the number of SN Ia events per year in the ICSP/IGSP can be given. The SN Ia event calculation is based on the estimate given by Blanc & Greggio (2008). For a given Salpeter IMF they calculate the fraction of SN Ia progenitors as a function of $M_\odot$, which is 0.022 $M_\odot^{-1}$ in our case. Furthermore they argue that 2–3% of these stars will give rise to a SN Ia event (we adopted 2.5%). After a stellar particle is formed in the simulations the SN Ia rate for this stellar particle is calculated with a fixed-time delay between the formation of the stellar particle and the SN Ia event of 1 Gyr. In Fig. 15 the SN Ia rate in units of SN Ia events per years in the ICSP for two different separation criteria (i.e. criterion 1 and criterion 2) is given. The amount of events correlates with the separation criteria. The number of events varies from 0.005 SN Ia to more than 0.1 SN Ia per year going off in the ICSP of the galaxy cluster. In the galaxy group system this number is nearly one magnitude lower for all separation criteria. As a SN Ia can heat their surrounding gas there might be an influence of SN Ia in the thermal component of the ICM or the inter-galactic medium (IGM). In Domainko et al. (2004)) this idea was discussed on estimates based on very few observations. In an upcoming work this idea will be investigated in more detail with simulations.

Assuming that one SN Ia releases in the surrounding medium on average 0.5 $M_\odot$ of ^{56}Ni (that becomes ^{56}Fr after radioactive decay) (Blanc & Greggio 2008), one can estimate the amount of iron introduced by SN Ia into ICM in the redshift interval $0 \leq z \leq 1$. In Table 3 the iron mass originating from SN Ia events in the ICSP for the different separation criteria are given. The maximum iron mass in the galaxy cluster originating from intergalactic SN Ia is of the order of 1×10^8 $M_\odot$. This value is almost two orders of magnitudes lower than observed in the

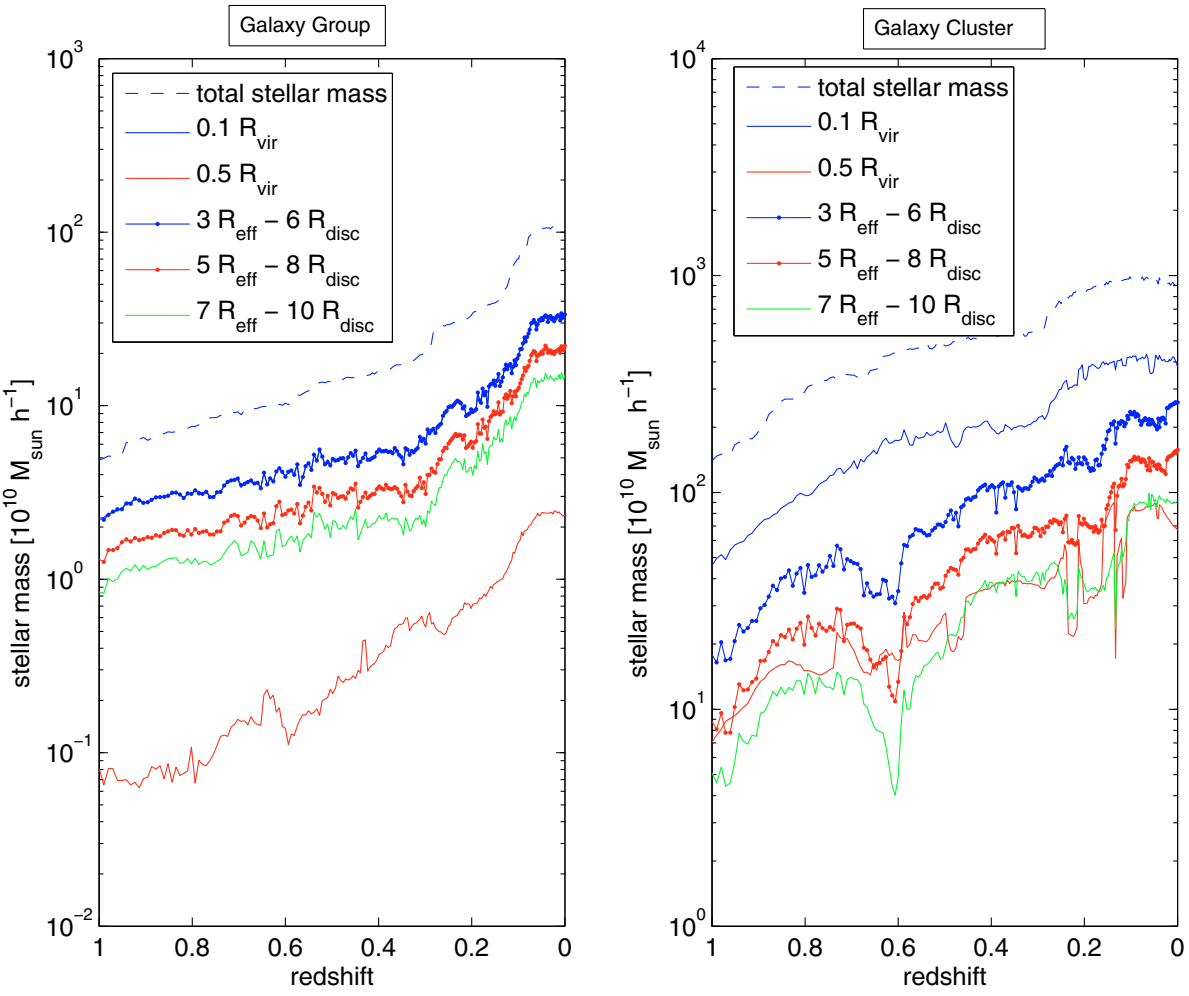

Fig. 10. Evolution of the stellar mass present in the intra-cluster/intra-group stellar population and the total stellar mass in the redshift range $0 \leq z \leq 1$ for different separation criteria.

ICM of galaxy clusters, which is of the order of 10^{10-12} $M_\odot$ iron mass (Arnaud et al. 1992). Taking all model assumptions into account we can conclude that SN Ia events in the ICSP are a less important enrichment mechanism compared to outflows by galactic winds and ram-pressure stripping (Domainko et al. 2007; Kapferer et al. 2007, 2009; Schindler et al. 2005; Tornatore et al. 2007).

6. The dynamics of the intra-cluster stellar population

As the ICSP/IGSP is located in the outer regions of the corresponding haloes, their velocity dispersion is smaller compared to the stellar population located in the centre of the structures. This can be seen in Figs. 16 and 17, where the evolution of the velocity dispersion of three different components in the two systems is shown, i.e. dark matter, stellar population and ICSP/IGSP (separation criterion 4). The main difference between the two systems is the difference of the velocity dispersion between the ICSP and the two other components in the galaxy cluster system compared to the group system. This reflects the higher interaction activity in the dense cluster environment, which shifts particles to larger radii from the centre for the dark matter haloes resulting in the different dynamics.

The imprint of halo-centric distances of particles belonging to the ICSP/IGSP and the stellar population located in the centre of the bound haloes can be seen in Fig. 18. The particles in the outskirts of the halo centres show a smoother distribution. In addition the maxima of the distributions of the different components are offset in the galaxy cluster simulation, again the ICSP components is not relaxed and more redistributed by many interactions than the IGSP component.
In principle it would be possible by comparing the velocity dispersion of the stellar component in the halo centres (i.e. galaxies) and the ICSP/IGSP to introduce a measure of how strong a system is affected by recent mergers of substructures. See Sommer-Larsen et al. (2005) for a spatial investigation of the dynamics of the diffuse stellar component in galaxy cluster and group simulations.

7. Discussion and conclusions

We investigated properties of the intra-cluster stellar population (ICSP) in a galaxy cluster and the intra-group stellar population

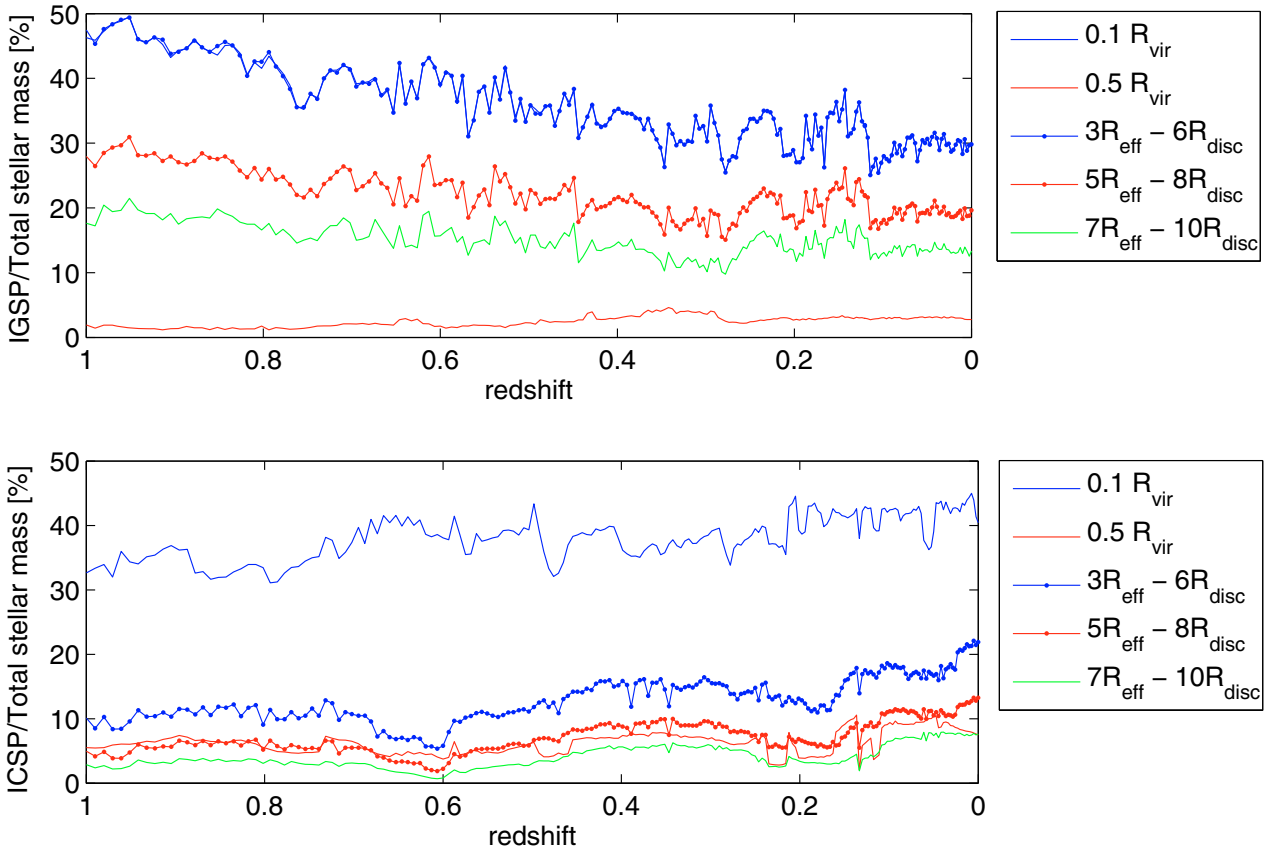

Fig. 11. Evolution of the ratio between the mass in the intra-cluster/intra-group stellar population to the total stellar mass in the redshift range $0 \leq z \leq 1$ for different separation criteria.

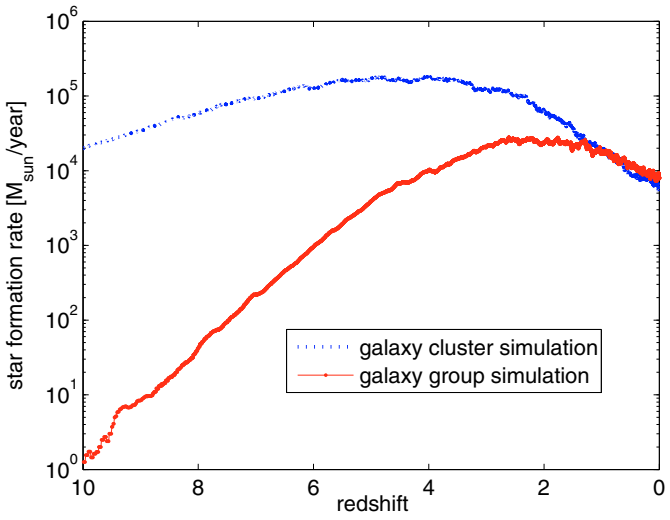

Fig. 12. Evolution of the star-formation rates in the whole cluster and group simulation volumes.

(IGSP) in a galaxy group system by means of combined *N*-body/smoothed particles hydrodynamic simulations including a recipe for star formation, feedback and cooling (Springel & Hernquist 2003). By applying different separation criteria between the stellar component residing in the centre of bound structures and the ICSP/IGSP (comparable to criteria applied by observers) we analysed the evolution of different properties of the resulting stellar populations and their dynamics. In addition we calculated SN Ia event rates in the ICSP/IGSP and their role in enriching the ICM/IGM. The underlying halo properties were extracted from our simulations by applying AHF (Knollmann & Knebe 2009). The results can be summarised as follows:

- Applying different separation criteria on the stellar component reveals different amounts of stellar mass present in the ICSP/IGSP. We find that 7% to 40% of all stars are belong to the ICSP in the galaxy cluster simulation at redshift $z = 0$ depending on the applied separation criteria. The same separation criteria applied on a group simulation results in a 3% to 30% IGSP component at redshift $z = 0$ compared to the total stellar mass in the system.
- There is a comparable amount of relative mass in the ICSP in our galaxy cluster simulation and IGSP in our galaxy group simulation.
- We found a major difference between the gradient in the evolution of the fraction of the ICSP and IGSP to the total stellar component. The fraction of ICSP in the galaxy cluster simulation increases little with decreasing redshift, whereas the fraction of stellar mass in the IGSP decreases with decreasing redshifts, although the virial mass in both systems increases in the same redshift interval. The dense, dynamical

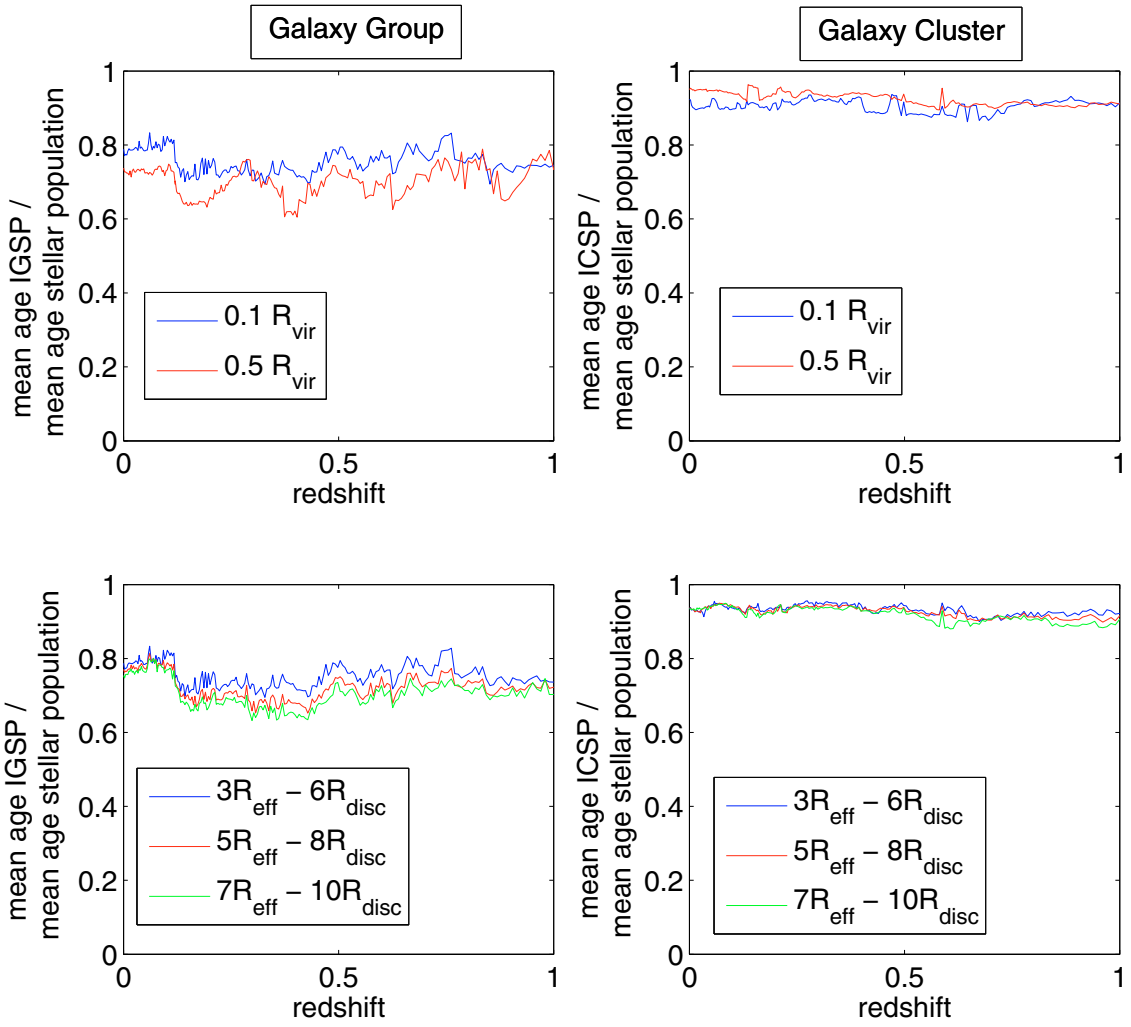

Fig. 13. Evolution of the ratio between the mean age of the intra-cluster stellar population to the mean age of the stellar population within the galaxies in the redshift range 0≤z≤ 1 for different separation criteria.

environment in galaxy cluster produces many high-velocity galaxy encounters which refill the ICSP perpetually. In the galaxy group system encounters are not as frequent and do not have as high relative velocities as in the galaxy cluster system, leading to a decrease in the fraction of IGSP to the total stellar population in the galaxy group system by violent relaxation.

- After each enhanced merger activity due to mass accretion of the systems an increase in the stellar mass present in the ICSP/IGSP can be found, which then decreases due to violent relaxation.
- The mean age of the stellar component present in the ICSP/IGSP is younger than the mean age of the stellar component present in the galaxies. For galaxy clusters the ICSP is on average 10% younger and the IGSP is on average 20% younger. Due to the high interaction rate with high relative velocities present in galaxy clusters stellar particles in the intergalactic regions do not violently relax at the same rate as in the galaxy group system.
- Applying simple SN Ia rate estimates on the simulated ICSP/IGSP gives SN Ia rates for the ICSP/IGSP of the order of 0.05 SN Ia events per year in the ICSP and one order of magnitude lower in the IGSP.
- The amount of ^{56}Fe-mass introduced by the ICSP SN Ia is nearly two orders of magnitudes lower then the observed values for the separation criterion, leading to the most pronounced ICSP.
- The velocity dispersion of the ICSP/IGSP and the stellar component in the galaxies shows similar evolution in the redshift regime $0 \leq z \leq 1$ for the galaxy cluster and the galaxy group system.
- The dispersion of the ICSP/IGSP is lower than that of the the stellar component in the galaxies. This reflects the location of the ICSP/IGSP at the outskirts of the haloes. In the galaxy cluster simulation the difference is more pronounced than in the galaxy group simulation, reflecting the higher kinematical energies involved in interactions in galaxy clusters compared to galaxy groups.
- The maximum in the velocity-dispersion distribution of the ICSP is shifted to lower velocities compared to the maximum in the velocity dispersion of the galaxies in the galaxy cluster. This reflects the high interaction rate and higher energetics of

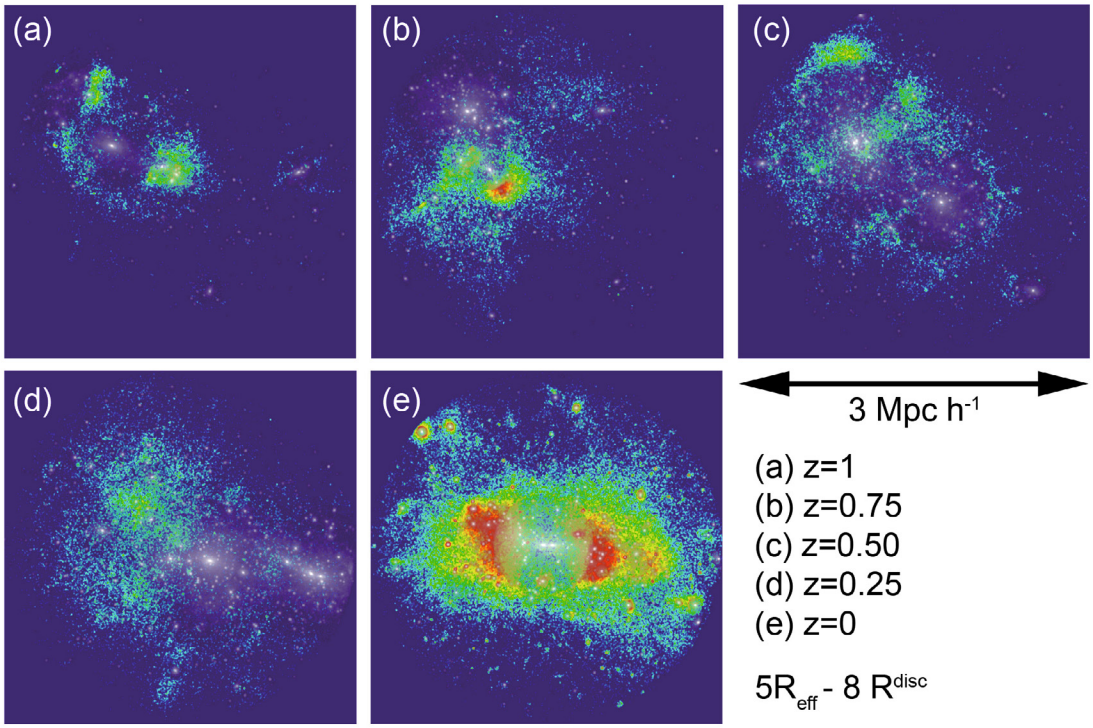

Fig. 14. Stellar surface-density for the intra-cluster stellar population (coloured map) and the stellar population in the galaxies (white to opaque colourmap) for different redshifts for the galaxy cluster system. The applied separation criterion is 5 $R_{\rm eff}$ for elliptical galaxies and 8 $R_{\rm disc}$ for spiral galaxies.

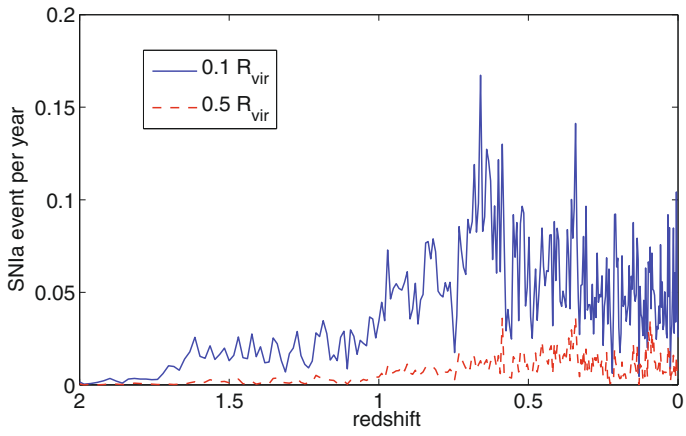

Fig. 15. Number of SN Ia events as a function of redshift in the intra-cluster stellar population for separation criterion 1 and criterion 2.

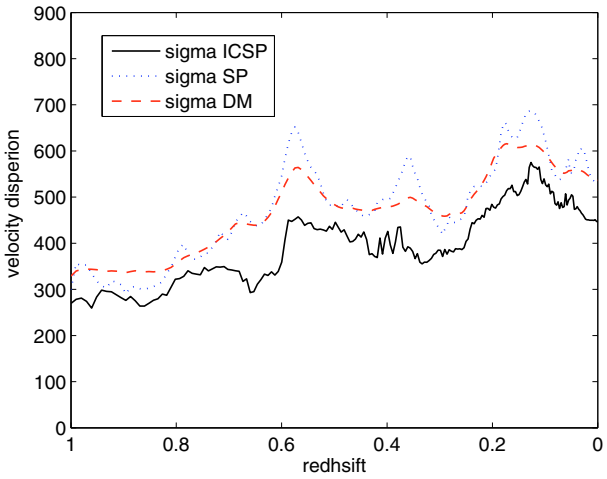

Fig. 16. Evolution of the velocity dispersion of the intra-cluster stellar population, the stellar population in the galaxies and the dark matter component in the redshift interval $0 \leq z \leq 1$ for the galaxy cluster system. The applied separation criterion is 5 $R_{\rm eff}$ for elliptical galaxies and 8 $R_{\rm disc}$ for spiral galaxies.

the interaction in galaxy clusters. As many stars of the ICSP populate the outskirts of haloes shortly after high interaction rates due to sub-cluster merger events, the magnitude of the difference gives us a measure for the dynamical state of the system. In the IGSP the difference is not as high due to the lower frequency of interactions and their lower relative interaction velocities compared to the galaxy cluster.

In principle ram-pressure stripping induced star formation in the wakes of cluster galaxies contributes to the ICSP. As the resolution of the simulation presented in this work is not high enough to resolve these processes in a self-consistent way, future very-high-resolution simulations will reveal the importance of this effect.

Although the detection of the ICSP/IGSP is at the limit of state-of-the-art observatories and many ideas and findings presented in this paper are beyond of what can be achieved with current observatories, in the future very deep observations of the ICSP/IGSP with next generation telescopes will help us to reveal

Table 3. ^{56}Fe mass originating from a SN Ia events in the ICSP/IGSP in the redshift interval $0 \leq z \leq 1$.

Crit.	Cluster	Group
1	4.1×10^8	2.9×10^7
2	7.7×10^7	2.2×10^6
3	2.0×10^8	4.4×10^7
4	1.2×10^8	2.3×10^7
5	6.4×10^7	1.4×10^7
Total stellar mass	1.19×10^{13}	1.13×10^{12}

Notes. Quantities are given in $M_\odot$ h^{-1}.

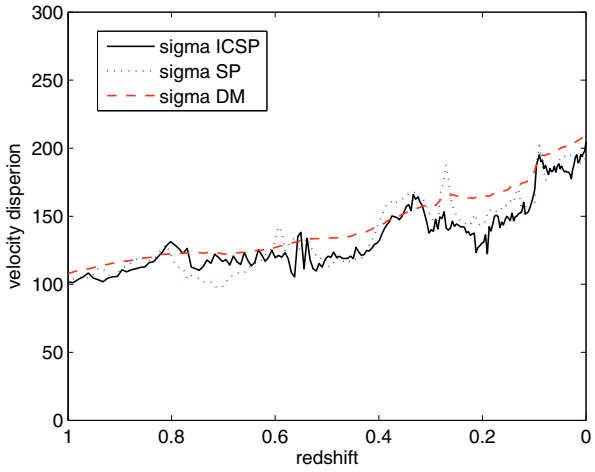

Fig. 17. Evolution of the velocity dispersion of the intra-group stellar population, the stellar population in the galaxies and the dark matter component in the redshift interval $0 \leq z \leq 1$ for the galaxy group system. The applied separation criterion is 5 $R_{\rm eff}$ for elliptical galaxies and 8 $R_{\rm disc}$ for spiral galaxies.

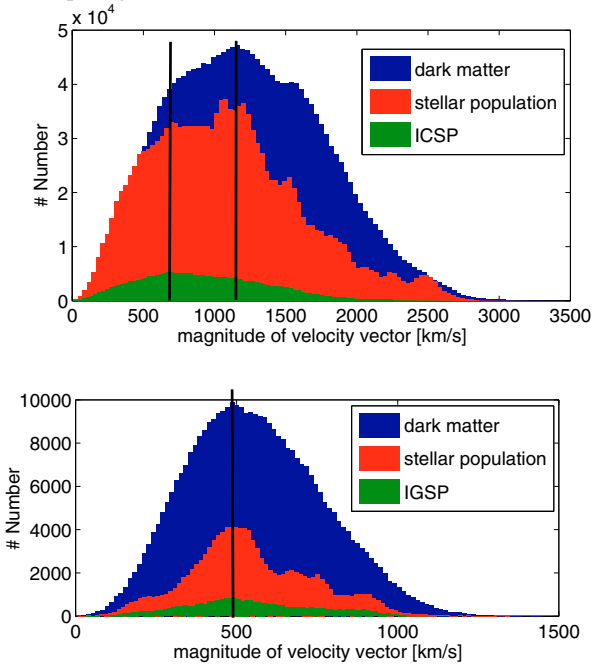

Fig. 18. Velocity distribution of the magnitude of the dark matter, stellar and ICSP/IGSP particles (separation criterion 4) in the galaxy cluster and group simulations in a 3 Mpc sphere around the cluster centre. The black vertical lines highlight the maximum in the dark matter and ICSP/IGSP components.

the evolution of systems like galaxy clusters and galaxy groups and their environmental influence on the evolution of galaxies.

Acknowledgements. The authors thank the anonymous referee who helped to improve the quality of the paper by many good suggestions. In addition the authors thank Volker Springel for GADGET-2 and Rien van de Weygaert and Ed Bertschinger for allowing us the use of their constrained random field code. S.R. Knollmann acknowledges support by the Ministerio de Ciencia en Innovacion (MICINN) under the Consolider-Ingenio, SyeC project CSD-2007-00050. The authors further acknowledge the UniInfrastrukturprogramm des BMWF Forschungsprojekt Konsortium Hochleistungsrechnen, the ESO Mobilitätsstipendien des BMWF (Austria), the Austrian Science Foundation (FWF) through grant P19300-N16, P18416, P18493, and the Tiroler Wissenschaftsfonds (Gefördert aus Mitteln des vom Land Tirol eingerichteten Wissenschaftsfonds).

References

Arnaboldi, M., Aguerri, J., Alfonso, L., et al. 2002, AJ, 123, 760
Arnaboldi, M., Freeman, K. C., Okamura, S., et al. 2003, AJ, 125, 514
Arnaboldi, M., Gerhard, O., Aguerri, J. A. L., et al. 2004, ApJ, 614, L33
Arnaud, M., Rothenflug, R., Boulade, O., Vigroux, L., & Vangioni-Flam, E. 1992, A&A, 254, 49
Burkert, A. M., & D'Onghia, E. 2004, Penetrating Bars Through Masks of Cosmic Dust, ed. D. L. Block, I. Puerari, K. C., Freeman, R. Groess, & E. K. Block, Astrophysics and space science library (ASSL), 319 (Dordrecht: Kluwer Academic Publishers), 341
Blanc, G., & Greggio, L. 2008, New Astron., 13, 606
Byrd, G., & Valtonen, M. 1990, ApJ, 350, 89
Chiosi, C., & Carraro, G. 2002, MNRAS, 335, 335
Da Rocha, C., Ziegler, B. L., & Mendes de Oliveira, C. 2008, MNRAS, 388, 1433
Domainko, W., Gitti, M., Schindler, S., et al. 2004, A&A, 425, L21
Domainko, W., Mair, M., Kapferer, W., et al. 2006, A&A, 452, 795
Feldmeier, J. J., Ciardullo, R., Jacoby, G. H., et al. 2003, ApJS, 145, 65
Gal-Yam, A., Maoz, D., Guhathakurta, P., et al. 2003, AJ, 125, 1087
Gerhard, O., Arnaboldi, M., Freeman, K. C., et al. 2005, ApJ, 621, L93
Gnedin, O. Y. 2003, ApJ, 589, 752
Hernquist, L., & Katz, N. 1989, ApJS, 70, 419
Hoffman, Y., & Ribak, E. 1991, ApJ, 380, L5
Kapferer, W., Knapp, A., Schindler, S., Kimeswenger, S., & van Kampen, E. 2005, A&A, 438, 87
Kapferer, W., Kronberger, T., Weratschnig, J., et al. 2007, A&A, 466, 813
Kapferer, W., Kronberger, T., Ferrari, C., Riser, T., & Schindler, S. 2008, MNRAS, 389, 1405
Kapferer, W., Sluka, C., Schindler, S., Ferrari, C., & Ziegler, B. 2009, A&A, 499, 87
Kapferer, W., Kronberger, T., Breitschwerdt, D., et al. 2009, A&A, 504, 719
Knollmann, S. R., & Knebe, A. 2009, ApJS, 182, 608
Krick, J. E., & Bernstein, R. A. 2007, AJ, 134, 466
Kronberger, T., Kapferer, W., Ferrari, C., Unterguggenberger, S., & Schindler, S. 2008, A&A, 481, 337
Lucy, L. B. 1977, AJ, 82, 1013
Merritt, D. 1984, ApJ, 276, 26
Mihos, J. C., Harding, P., Feldmeier, J., et al. 2005, ApJ, 631, L41
Gingold, R. A., & Monaghan, J. J. 1977, MNRAS, 181, 375
Moles, M., Marquez, I., & Sulentic, J. W. 1998, A&A, 334, 473
Moore, B., Katz, N., Lake, G., Dressler, A., & Oemler, A. 1996, Nature, 379, 613
Murante, G., Arnaboldi, M., Gerhard, O., et al. 2004, ApJ, 607, L83
Murante, G., Giovalli, M., Gerhard, O., et al. 2007, MNRAS, 377, 2
Napolitano, N. R., Pannella, M., Arnaboldi, M., et al. 2003, ApJ, 594, 172
Nishiura, S., Murayama, T., Shimada, M., et al. 2000, AJ, 120, 2355
Rudick, C. S., Mihos, J. C., & McBride, C. 2006, ApJ, 648, 936
Schindler, S., Kapferer, W., Domainko, W., et al. 2005, A&A, 435, L25
Sommer-Larsen, J., Romeo, A. D., & Portinari, L. 2005, MNRAS, 357, 478
Sommer-Larsen, J. 2006, MNRAS, 369, 958
Springel, V., & Hernquist, L. 2003, MNRAS, 339, 312
Springel, V. 2005, MNRAS, 364, 1105
Sulentic, J. W., & Lorre, J. J. 1983, A&A, 120, 36
Tornatore, L., Borgani, S., Dolag, K., et al. 2007, MNRAS, 382, 1050
van de Weygaert, R., & Bertschinger, E. 1996, MNRAS, 281, 84
Willman, B., Governato, F., Wadsley, J., et al. 2004, MNRAS, 355, 159
White, P. M., Bothun, G., Guerrero, M. A., et al. 2003, ApJ, 585, 739
Zibetti, S., White, S. D. M., Schneider, D. P., et al. 2005, MNRAS, 358, 949